

Microbial-Induced Heterogeneity in the Acoustic Properties of Porous Media

Caroline A. Davis¹, Laura J. Pyrak-Nolte², Estella A. Atekwana^{3*},
D. Dale Werkema Jr.⁴ and Marisa E. Haugen²

1. *Missouri University of Science and Technology, Rolla, MO 65409*
2. *Purdue University, West Lafayette, IN 47907*
3. *Oklahoma State University, Stillwater, OK 74078*
4. *U.S. Environmental Protection Agency, Las Vegas, NV 89119*

Corresponding author: Tel.: +1 405 744 6358; Fax: +1 405 744 7841

Email address: estella.atekwana@okstate.edu

Abstract

It is not known how biofilms affect seismic wave propagation in porous media. Such knowledge is critical for assessing the utility of seismic techniques for imaging biofilm development and their effects in field settings. Acoustic wave data were acquired over a two-dimensional region of a microbial-stimulated sand column and an unstimulated sand column. The acoustic signals from the unstimulated column were relatively uniform over the 2D scan region. The data from the microbial-stimulated column exhibited a high degree of spatial heterogeneity in the acoustic wave amplitude, with some regions exhibiting significant increases in attenuation while others exhibited decreases. Environmental scanning electron microscopy showed differences in the structure of the biofilm between regions of increased and decreased acoustic wave amplitude. We conclude from these observations that variations in microbial growth and biofilm structure cause heterogeneity in the elastic properties of porous media with implications for the validation of bioclogging models.

INDEX TERMS: 5102 Acoustic properties, 0416 Biogeophysics, 0463 Microbe/mineral interactions.

1.0 Introduction

Bioclogging caused by biofilm development is a phenomenon that can cause significant changes in the physical properties of porous media including porosity and permeability changes that influence fluid flow and transport properties [e.g., *Baveye et al.*, 1998] and remediation efforts. Numerical models and simulations have been developed to qualitatively forecast the change in hydraulic properties of a porous medium from bioclogging [e.g., *Brovelli et al.*, 2009]. Bioclogging processes are dynamic and are influenced by many phenomena including initial heterogeneities in biomass distribution as well as the physical properties of the porous medium [e.g., *Brovelli et al.*, 2009]. A major difficulty inherent with experimental modeling approaches is that *in situ* quantitative information from direct observation of biological growth and clogging from field data is difficult to obtain at the appropriate spatiotemporal scales needed for model validation [*Dupin and McCarty*, 2000]. Minimally invasive diagnostic techniques are needed to provide near real-time information of the spatiotemporal distribution of biofilms in porous media for validating predictive models and for monitoring microbial growth *in situ*. Although several studies have investigated the rheological properties of biofilms in laboratory settings [e.g., *Stoodley et al.*, 1999], it is not known how biofilms affect seismic wave propagation in porous media. Such an understanding is critical for assessing the utility of seismic techniques for imaging biofilm spatial heterogeneity and their effects on porous media in field settings.

To date, most biogeophysical investigations have focused on geoelectrical techniques [*Atekwana et al.*, 2006]. Apart from a few studies [e.g., *Williams et al.*, 2005; *DeJong et al.*, 2006], less attention has been given to the effects of microbial interactions with geologic media on elastic properties, hence questions remain about the effect of microbial growth and biofilm formation in porous media on acoustic wave propagation in the absence of biomineralization. The work described in this letter investigates the influence of biofilm formation on the

spatiotemporal seismic properties of porous media. We show for the first time that variations in biofilm structure/texture cause heterogeneity in acoustic wave attenuation of porous media.

2.0 Materials and Methods

Prismatic experimental columns, measuring 102 mm by 51 mm by 254 mm (width x depth x height), were fabricated using 3.2 mm thick clear acrylic. The columns were wet-packed with coarse grain (0.6-1.18 mm) ASTM 20/30 silica sand (Ottawa, IL). Prior to packing, the sands were washed with deionized (DI) water and disinfected by autoclaving. Columns and accessory equipment were also disinfected by rinsing with a 70% ethanol solution. Prior to saturation with the experimental fluids, the sand-packed columns were saturated with sterile 25% Bushnell Haas (BH) nutrient broth (Becton Dickinson) and baseline acoustic measurements were recorded. After initial background measurements, microbial growth was stimulated in one sand column (biostimulated column) by saturating with 25% BH nutrient broth, 30 mM glucose, *Pseudomonas aeruginosa* PAO1 wild type bacteria culture, and 30 µg/mL Gentamicin antibiotic. The bacteria strain (specifically PAO1 Tn7-Gm-gfp) was obtained from the University of Denmark (Lyngby, Denmark), where previous studies with this bacteria strain have been conducted [e.g., Pamp and Tolker-Nielsen, 2007]. The other column (unstimulated column) was used for background measurements and was saturated with 25% BH and Gentamicin antibiotic. The Gentamicin antibiotic was added to both the biostimulated and unstimulated columns to inhibit the growth of microorganisms other than the *P. aeruginosa* in the biostimulated column.

2.1 Acoustic Wave Measurements

A full-waveform acoustic wave imaging system was used to obtain two-dimensional point-by-point maps of the acoustic response of the samples [e.g., Acosta-Colon *et al.*; 2009]. The acoustic imaging system used two water-coupled plane-wave transducers (1 MHz central frequency) for

the source and receiver. The columns were placed in a water tank to a depth $\frac{2}{3}$ the length of a column, and remained *in situ* at laboratory temperature (22-24 °C) for the duration of the experiment. Using the acoustic mapping mode (C-scan), computer-controlled linear actuators (Newport 850-B4 and Motion Master 2000) were used to move the source and receiver in unison over a 60 mm by 70 mm region in 5 mm increments. A pulse generator (Panametrics PR1500) was used to excite the source and to receive the transmitted signal from the receiver. At each point in the 2D scan region, a 100 microsecond window of the transmitted signal was recorded and digitized with an oscilloscope (Lecroy 9314L). The entire 2D region was scanned 2-3 times per week for the 29 day duration of the experiment.

2.2 Sampling and Analyses

Fluid samples were collected 1-2 times per week from the bottom valve of the columns. The pH was measured using a bench-top probe immediately after fluids were withdrawn. Upon termination of the experiment, the columns were destructively sampled by withdrawing cores of the wet sand (core diameter ~ 6 mm) in a grid-like fashion (15 mm by 15 mm grid) from the acoustic scan region. The sand cores were used for environmental scanning electron microscopy (FEI Quanta 600 ESEM) to image and characterize the surfaces of the sand grains.

3.0 Results

3.1 Acoustic Wave Monitoring

A time-frequency analysis [Nolte *et al.*, 2000] was performed to determine the amplitude of the compressional signal at a frequency of 0.5 MHz, i.e., the most probable or dominant frequency of the signals. The 2D acoustic scan images of the transmitted compressional wave amplitude obtained from the biostimulated and unstimulated columns are shown in Figure 1, and the temporal percent change in acoustic wave amplitude relative to Day 1 is shown in Figure 2. The

2D scans obtained from the biostimulated column on Day 1 reveal relatively uniform compressional wave amplitude over the scan region. However, by Day 5 significant changes were observed in the biostimulated column and the average amplitudes varied spatially over the scan region. For the biostimulated column, the 2D image obtained on Day 29 exhibited an increase in amplitude in some regions (i.e., Figure 1a; Location A), while other regions showed a decrease in amplitude (i.e., Figure 1a; Location B). This is clearly observed in Figure 2a. Unlike the unstimulated column (Figure 2b), the change in amplitude as a function of time varied with location for the biostimulated column (Figure 2a). Compared to Day 1, locations A-C in the biostimulated column (Figure 2a) initially show a decrease in amplitude of ~40% to Day 5. Thereafter, the amplitudes at locations A and B in the biostimulated column increased reaching initial baseline amplitudes by Day 10. The amplitude at location C also increased after Day 5 but did not return to baseline values. Locations D and E (Figure 2a) show a decrease in amplitudes of ~80% by Day 14 and remain relatively steady to the end of the experiment. The relatively small overall variation in amplitude (<20%) relative to Day 1 observed from the unstimulated column is consistent for all of the select data points plotted (Figure 2b; Locations A-E).

3.2 Geochemical Monitoring

The pH values from the biostimulated column steadily decreased from a baseline pH of 7 to near 4.4 on Day 12, and remained at a pH of 4.4 through Day 20 (data not shown). From the unstimulated column, a pH of 7 was consistent throughout the duration of the experiment.

3.3 Sand Surface Imaging

Representative ESEM images from the columns sampled at the end of the experiment are shown on Figure 1c. Samples from an area of increased acoustic amplitude (location A, Figure 1a) in the biostimulated column shows a rough textured surface which appears to have a patchy

covering of 'biomaterial' over some portions of the sand grain, while on other portions of the image the silica sand surface is clearly visible (panel A, Figure 1c). Rod-shaped bacterial cells are present in this biomaterial, but not clearly distinguishable in this image. The ESEM images of sand sampled from an area of decreased acoustic amplitude (location B, Figure 1a) in the biostimulated column show the surface of a sand grain which appears to be completely covered in a smooth biomaterial, with several holes and void-spaces (panel B, Figure 1c). This image also shows the presence of attached rod-shaped bacteria embedded in this biomaterial. In contrast, the ESEM images of samples obtained from the unstimulated column (location C, Figure 1B) show the irregular or hummocky surface of a silica sand grain with no apparent attached bacteria cells or biomass (panel C, Figure 1c).

4.0 Discussion and Conclusions

In this study the compressional wave amplitude was observed to differ both temporally and spatially, between the biostimulated and unstimulated columns (Figure 1). Compressional wave amplitudes in the biostimulated column became more spatially variable while the acoustic response of the unstimulated column homogenized over time. While the changes observed in the unstimulated column (<20%) are not insignificant (Figure 2b), they are far less than the measured changes from the biostimulated column and consistent for all of the select data points. Hence we attribute the changes in the latter to particle settling. Except for a few locations (e.g., Location A, Figures 1a & 2a) that showed an increase, most locations in the biostimulated column showed a decrease in the compressional wave amplitudes over time with some regions decreasing to ~ 80% of Day 1 values (e.g., Location E, Figure 2a). Microbial growth was active in the biostimulated column as evidenced by the decrease in pH (from 7 to 4.4) and ESEM images that confirm microbial cell colonization of sand surfaces (Figure 1c, panels A and B). No

microbial growth was observed in the unstimulated column (panel C, Figure 1c). The decrease in pH most likely resulted from the accumulation of metabolic byproducts such as organic acids [e.g., *Silverman and Munoz*, 1974], which eventually inhibited continued microbial growth in the columns.

The bacteria culture used in this study (*P. aeruginosa*) is capable of producing different types of biofilms, depending on the environment [e.g., *Friedman and Kolter*, 2004], and formation of these biofilms is documented to occur in different stages [e.g., *Davey et al.*, 2003]. Initial stages in the formation of *P. aeruginosa* biofilms are characterized by the attachment of planktonic cells to solid surfaces. Initial attachment is followed by colonization of the surfaces followed by the production of extrapolymer substances (alginate - a viscous gum) that embed the reproducing cells allowing them to form microcolonies and build thick biofilms. One characteristic of the *P. aeruginosa* biofilms described in the literature [e.g., *Davey et al.*, 2003; *Pamp and Tolker-Nielsen*, 2007] is the presence of macrocolonies surrounded by large void spaces or open, dark fluid-filled channels, through which the lower levels of bacteria in the biofilm are thought to dispose of accumulating waste products (e.g., see panel B, Figure 1c). The ESEM images (panel A and B, Figure 1c) obtained from the biostimulated column show apparent qualitative differences in the texture of the attached biofilm between areas of increased and decreased amplitude. We hypothesize that differences in the measured amplitudes reflect differences in the structure/texture of the attached biofilms in the biostimulated column.

Acoustic properties of porous media are generally dependant on the bulk modulus of the saturating fluid [e.g., *Knight and Nolen-Hoeksema*, 1990], the elastic moduli of the solid media [e.g., *Ecker et al.*, 1998], and the solid-fluid interactions [e.g., *Clark et al.*, 1980]. Energy loss mechanisms for fluid-saturated porous media fall into three categories: viscoelastic loss, fluid-

solid surface physiochemical loss, and scattering loss [Li *et al.*, 2001]. Generally, decreases in acoustic amplitude result from biogenic gas production or the weakening of grain contacts (physical/chemical alteration of surfaces and/or grain contacts [e.g., Murphy *et al.*, 1984; Clark *et al.*, 1980]) in porous media, both of which reduce the elastic moduli and are manifested by delays and attenuation of acoustic waves. We observed no gas bubble formation in the biostimulated column. Hence, we hypothesize that the presence of biofilms caused the changes in elastic properties of the sample which is consistent with studies that suggest that soft and patchy structures like biofilm surfaces result in the effective attenuation of sound [e.g., Janknecht and Melo, 2003].

Increases in acoustic amplitude may result from increases in the bulk modulus of the solid media [e.g., Li *et al.*, 2001] through the stiffening of grain contacts. Hence it is possible that in the regions of increased amplitude, the extrapolymer substances resulted in enhanced coupling between grains, whereas areas of decreased amplitude may be explained by viscous losses or physiochemical alterations at grain contacts due to the nature of the biofilms. We note that during ESEM imaging of the sand samples from regions with increased amplitude (Figure 1a; Location A), individual bacterial cells were not clearly distinguishable until the operating temperature of the ESEM was raised from 5 to 20°C, and the relative humidity was decreased from 89% to 14%, which effectively dried out the sample/biomaterial. However, individual cells and attached biomass on sand samples collected from Location B (Figure 1a), were evident immediately upon viewing with the ESEM (at 5°C and 89%) and remained virtually the same in appearance when the temperature was increased to 20°C (images not shown).

Wave scattering or interference from spatial heterogeneity of the medium is another mechanism that affects wave attenuation. The biostimulated sample did not exhibit biogenic gas

formation, which suggests that air bubbles are not a source of scattering. The density contrast between water-saturated sediment and the biofilm-microbially altered sediment is not large. Thus, a potential source of scattering is a spatial variation in elastic or viscoelastic moduli from microbial alteration of the grain contact, pore-filling material and/or biofilm connecting grains.

Our investigation shows that acoustic imaging techniques are sensitive to spatiotemporal changes in porous media caused by enhanced microbial growth of a biofilm forming bacteria culture. While the exact microbial-induced mechanisms for the variations in amplitude are yet unclear, we speculate that the differences in amplitude arise from a non-uniform distribution of microbial activity or possible heterogeneity in the biomass distribution and biofilm morphology. The applicability of our laboratory measurements to the field scale will depend on spatial and temporal dispersion. Temporal dispersion connects frequency-dependent attenuation and velocity with elastic moduli, i.e. changes at grain contacts or pore-filling. Spatial dispersion connects wavelength with the size of the scatterer, i.e., the size and/or spatial correlation length of microbially altered regions. Increasing or decreasing attenuation with frequency will provide information on the size of the altered region and on the spatiotemporal distribution of biomass/bioclogging development.

Acknowledgements

This material is based in part on work supported by the National Science Foundation under Grant No. OCE-0729642, EAR 0722410 (MRI), EAR 0525316, and REU Award # 0552918, EPA Student Services Contract EP07D000660, Office of Basic Energy Sciences, US Department of Energy (DEFG02-97ER14785 08). S. Pamp and T. Tolker-Nielsen provided the *Pseudomonas* PAO1 Tn7-Gm-gfp strain to S. Rossbach, and we thank S. Rossbach for helpful discussions on culturing the bacteria. Although this work was reviewed by EPA and approved

for presentation, it may not necessarily reflect official Agency policy. Mention of trade names or commercial products does not constitute endorsement or recommendation by EPA for use.

References

- Acosta-Colon, A., L. J. Pyrak-Nolte, and D. D. Nolte (2009), Laboratory-scale study of field of view and the seismic interpretation of fracture specific stiffness, *Geophys. Prospect.*, 57(2), 209-224.
- Atekwana, E. A., E. A. Atekwana, and D.D. Werkema (2006), Biogeophysics: the effects of microbial processes on geophysical properties of the shallow subsurface, in *Applied Hydrogeophysics*, edited by H. Vereecken, A. Binley, G. Cassiani, A. Revil, and K. Titov, pp. 161-193, NATO Sci. Ser. IV, Springer, New York.
- Baveye, P., P. Vandevivere, B. L. Hoyle, P. C. DeLeo, and D. Sanchez de Lozada, (1998), Environmental impact and mechanisms of the biological clogging of saturated soils and aquifer materials, *Crit. Rev. Environ. Sci. Tech.*, 28(2), 123-191.
- Brovelli, A., F. Malaguerra, and D. A. Barry, (2009), Bioclogging in porous media: Model development and sensitivity to initial conditions, *Environmental Modelling and Software*, 24, 611-626.
- Clark, V. A., B. R. Tittman, and T. W. Spencer, (1980), Effect of volatiles on attenuation (Q-1) and velocity in sedimentary rocks, *J. Geophys. Res.*, 85, 5190-5198.
- Davey, M. E., N. C. Caiazza, and G. A. O'Toole (2003), Rhamnolipid surfactant production affects biofilm architecture in *Pseudomonas aeruginosa* PAO1, *J. Bacteriol.*, 185(3), 1027-1036, doi:10.1128/JB.185.3.1027-1036.2003.
- DeJong, J. T., M. B. Fritzges, and K. Nusslein (2006), Microbially induced cementation to control sand response to undrained shear, *J. Geotech. Geoenviron. Eng.*, 132(11), 1381-1392.

- Dupin, H. J., and P. L. McCarty (2000), Impact of colony morphologies and disinfection on biological clogging in porous media, *Environ. Sci. Technol.*, 34(8), 1513-1520; doi:10.1021/es990452f.
- Ecker, C., J. Dvorkin, and A. Nur (1998), Sediments with gas hydrates: internal structure from seismic AVO, *Geophysics*, 63, 1659-1669.
- Friedman, L., and R. Kolter (2004), Genes involved in matrix formation in *Pseudomonas aeruginosa* PA14 biofilms, *Molec. Microbio.*, 51(3), 675–690 doi:10.1046/j.1365-2958.2003.03877.x.
- Janknecht , P and L. F. Melo (2003), Online biofilm monitoring, *Rev. in Env. Sci. and Bio/Techn.*, 2, 269–283.
- Knight, R., and R. Nolen-Hoeksema, (1990), A laboratory study of the dependence of elastic wave velocities on pore scale fluid distribution, *Geophys. Res. Lett.*, 17, 1529-1532.
- Li, X., L. R. Zhong, and L. J. Pyrak-Nolte (2001), Physics of partially saturated porous media: residual saturation and seismic-wave propagation, *Ann. Rev. Earth Planet. Sci.*, 29, 419-460.
- Murphy III, W. F., K. W. Winkler, and R. L. Kleinberg (1984), Frame modulus reduction in sedimentary rocks: the effect of adsorption on grain contacts, *Geophys. Res. Lett.*, 1(9), 805-808.
- Nolte, D. D., L. J. Pyrak-Nolte, J. Beachy, and C. Ziegler (2000), Transition from the displacement discontinuity limit to the resonant scattering regime for fracture interface waves, *International Journal of Rock Mechanics and Mining Sciences*, 37(1-2), 219-230.
- Pamp, S. J., and T. Tolker-Nielsen (2007), Multiple roles of biosurfactants in structural biofilm development by *Pseudomonas aeruginosa*, *J. Bacteriol.*, 189(6), 2531–2539, doi:10.1128/JB.01515-06.

Silverman, M. P., and E. F. Munoz (1974), Microbial metabolism and dynamic changes in the electrical conductivity of soil solutions: A method for detecting extraterrestrial life, *Appl. Microbiol.*, 28(6), 960– 967.

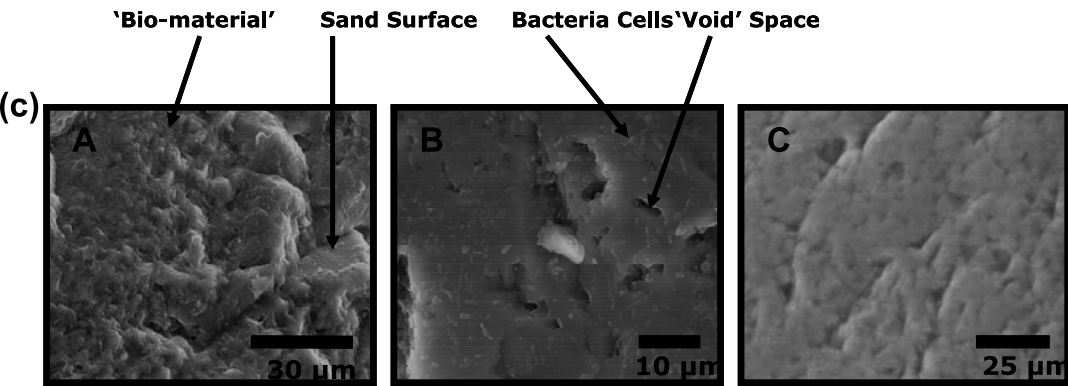
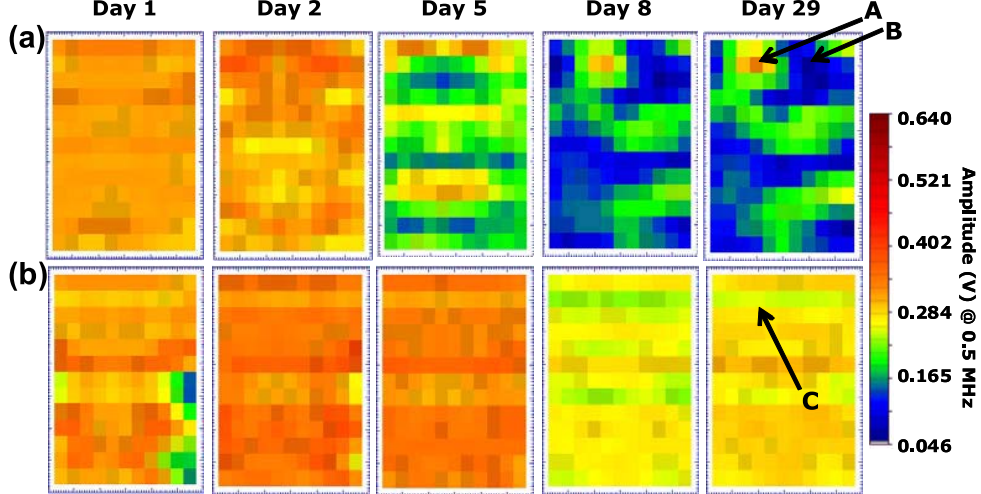
Stoodley, P., Z. Lewandowski, J. D. Boyle, and H. M. Lappin-Scott (1999), Structural deformation of bacterial biofilms caused by short-term fluctuations in fluid shear: an in situ investigation of biofilm rheology, *Biotech. Bioeng.*, 65(1), 83-92.

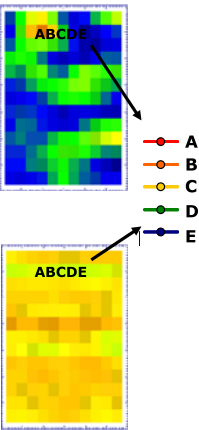
Williams, K. H., D. Ntarlagiannis, L. D. Slater, A. Dohnalkova, S. S. Hubbard, and J. F. Banfield, (2005), Geophysical imaging of stimulated microbial biomineralization, *Environ. Sci. Technol.*, 39(19), 7592-7600.

Figure Captions

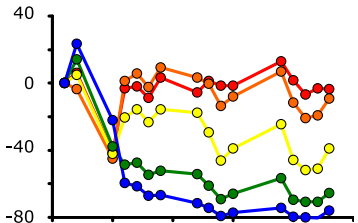
Figure 1: 2D acoustic wave amplitude scans (at 0.5 MHz) from the (a) biostimulated and (b) unstimulated columns for Days 1, 2, 5, 8, and 29. Black letters (A,B,C) on Day 29 of the 2D scans denotes location of ESEM images shown in (c): panel (A) is from the biostimulated column from an area of increased amplitude; panel (B) is from an area of decreased amplitude; and panel (C) is from the unstimulated column with no apparent attached biomass. Note the differences in the texture of the attached biomass between (A) having a rough texture and (B) smooth texture with the grain surfaces completely covered by biomaterial.

Figure 2: Graphs showing the temporal percent change in acoustic wave amplitude (at 0.5 MHz) relative to Day 1 for the (a) biostimulated and (b) unstimulated columns. Note the significant increase in attenuation (~80 %) for the biostimulated compared to the unstimulated sample (~20 %).





(a) % Change Amplitude (relative to Day 1)



(b) % Change Amplitude (relative to Day 1)

